strengthening of neuronal connections during the detection and storage of new information by the hippocampus. □

Methods

Electrode implantation and electrophysiology. Experiments were carried out on freely behaving male Wistar rats (200–300 g) that had electrodes implanted under pentobarbitone (60 mg kg^{-1}) anaesthesia. Recordings of field EPSPs were made from the CA1 stratum radiatum of the hippocampus in response to ipsilateral stimulation of the Schaffer collateral/commissural pathway using techniques similar to those described[26,27]. Animals recovered at least 14 days before the start of the experiment. Test EPSPs were evoked at a frequency of 0.033 Hz and at a stimulation intensity adjusted to give an EPSP amplitude of 50% of maximum. The high-frequency stimulation protocol for inducing LTP consisted of 10 trains of 20 stimuli, interstimulus interval 5 ms (200 Hz), intertrain interval, 2 s. Repeated stimulation with this protocol fails to increase the magnitude of LTP, indicating that it is almost at saturation for the group of synapses under observation[26]. LTP was measured as mean ± s.e.m.% of baseline EPSP amplitude recorded over at least a 20-min baseline period. The EEG was simultaneously monitored (from the hippocampal recording electrode) during all experiments so as to ensure that no abnormal activity was evoked by the conditioning stimulation and to monitor hippocampal theta EEG activity. The spectral power of the EEG was measured after fast Fourier transformation of sweeps of 1.2 s duration. Dual pathway experiments, with two independent ipsilateral stimulation inputs to the same recording electrode, were carried out for most experiments. Lack of paired-pulse interaction with responses evoked in the test pathway was used as a criterion of independence.

Recording apparatus and novelty exploration. To allow free exploration without extensive locomotion (which affects brain temperature and field potential measures of synaptic transmission[4,6,28,29], the recording boxes were relatively small (0.07 or 0.08 m^2). Under these conditions, only very transient (<10 min) and small changes (<1 °C) in brain temperature were observed on entering the novel environment.

Experiments were carried out in a well lit (~750 lux, fluorescent lighting) room. The familiar box was made of clear perspex, whereas the novel box was made of Perspex covered with a thin sheet of plastic which acted as a red filter (>600 nm, filter factor ~3×). The boxes in the first study had different shapes (34 × 24 × 24 cm for the familiar, versus 32 × 21 × 20 cm for the novel box). In the other studies, an opaque barrier that separated the familiar and novel environments was removed at 90 min and was closed 20 min later when the animal was in the novel box. To make the novel environment more distinct, the bedding was also different (none in the familiar, versus wood shavings in the novel box). The bedding was changed between rats but was not changed after each trial for a given rat. Behavioural evidence that the animals acquired information about the new environment was provided by the observation that the animals explored less on re-exposure to the novel box on consecutive days (for example, 24 ± 6 versus 14 ± 4 transitions between the familiar and novel boxes in the first 20 min on the first and third day, respectively; $P < 0.05$). Entry into the novel box did not elicit any observable stress responses either hormonally (plasma corticosterone, 5.2 ± 1.2 versus 3 ± 0.8 μg dl^{-1} in familiar box, measured by HPLC; $n = 4$)[27] or behaviourally (no evidence of behavioural freezing, piloerection or defecation typical of stress). The animals were housed individually in their home cage between recording sessions. Statistical comparisons were made by using Friedman two-way analysis of variance by ranks and Mann–Whitney *U*-test where appropriate.

Received 20 March; accepted 9 June 1998.

1. Martinez, J. & Derrick, B. Long-term potentiation and learning. *Annu. Rev. Psychol.* 47, 173–203 (1996).
2. Jeffery, K. LTP and spatial learning—Where to next? *Hippocampus* 7, 95–110 (1997).
3. Morris, R. G. M. & Frey, U. Hippocampal synaptic plasticity: role in spatial learning or the automatic recording of attended experience? *Phil. Trans. R. Soc. Lond. B* 352, 1489–1503 (1997).
4. Hargreaves, E. L., Cain, D. P. & Vanderwolf, C. Learning and behavioral long-term potentiation: importance of controlling for motor activity. *J. Neurosci.* 10, 1472–1478 (1990).
5. Brickson, C. A., McNaughton, B. L. & Barnes, C. A. Competition of long-term enhancement and short-term exploratory modulation of perforant path synaptic transmission. *Brain Res.* 615, 275–280 (1993).
6. Moser, E., Moser, M.-B. & Andersen, P. Potentiation of dentate synapses initiated by exploratory learning in rats: dissociation from brain temperature, motor activity, and arousal. *Learning Memory* 1, 53–73 (1994).
7. Abraham, W. C. & Bear, M. F. Metaplasticity: the plasticity of synaptic plasticity. *Trends Neurosci.* 19, 126–130 (1996).
8. O'Keefe, J. & Nadel, L. *The Hippocampus as a Cognitive Map* (Clarendon, Oxford, 1978).
9. Eichenbaum, H. Is the rodent hippocampus just for 'place'? *Curr. Opin. Neurobiol.* 6, 187–195 (1996).
10. Green, J. & Arduini, A. Hippocampal electrical activity in arousal. *J. Neurophysiol.* 17, 533–557 (1954).
11. Bland, B. The physiology and pharmacology of hippocampal formation theta rhythms. *Progr. Neurobiol.* 26, 1–54 (1986).
12. Buzsáki, G. Two stage model of memory trace formation: a role for noisy brain states. *Neuroscience* 31, 551–570 (1989).
13. Huang, Y.-Y., Nguyen, P., Abel, T. & Kandel, E. Long-lasting forms of synaptic potentiation in the mammalian hippocampus. *Learning Memory* 3, 74–85 (1996).
14. Staubli, U. & Lynch, G. Stable depression of potentiated synaptic responses in the hippocampus with 1–5 Hz stimulation. *Brain Res.* 513, 113–118 (1990).
15. Doyle, C. A., Cullen, W. K., Rowan, M. J. & Anwyl, R. Low-frequency stimulation induces homosynaptic depotentiation but not long-term depression of synaptic transmission in the adult anaesthetized and awake rat hippocampus *in vivo*. *Neuroscience* 77, 75–85 (1997).
16. Manahan-Vaughan, D. Group 1 and 2 metabotropic glutamate receptors play differential roles in hippocampal long-term depression and long-term potentiation in freely moving rats. *J. Neurosci.* 17, 3303–3311 (1997).
17. Errington, M. L. *et al.* Stimulation at 1–5 Hz does not produce long-term depression or depotentiation in the hippocampus of the adult rat *in vivo*. *J. Neurophysiol.* 74, 1793–1799 (1995).
18. Huerta, P. & Lisman, J. Bidirectional synaptic plasticity induced by a single burst during cholinergic theta oscillation in CA1 *in vitro*. *Neuron* 15, 1053–1063 (1995).
19. Staubli, U. & Chun, D. Factors regulating the reversibility of long-term potentiation. *J. Neurosci.* 16, 853–860 (1996).
20. Parkin, A. J. Human memory: novelty, association and the brain. *Curr. Biol.* 7, R768–R769 (1997).
21. Grunwald, T., Lehnertz, K., Heinze, H. J., Helmstaedter, C. & Elger, C. E. Verbal novelty detection within the human hippocampus proper. *Proc. Natl Acad. Sci. USA* 95, 3195–3197 (1998).
22. Honey, R. C., Watt, A. & Good, M. Hippocampal lesions disrupt an associative mismatch process. *J. Neurosci.* 18, 2226–2230 (1998).
23. Gluck, M. & Myers, C. Psychobiological models of hippocampal function in learning and memory. *Annu. Rev. Psychol.* 48, 481–514 (1997).
24. Miller, K. Synaptic economics: competition and cooperation in synaptic plasticity. *Neuron* 17, 371–374 (1996).
25. Dudai, Y. Consolidation: fragility on the road to the engram. *Neuron* 17, 367–370 (1996).
26. Doyle, C., Hoibeches, C., Rowan, M. J. & Anwyl, R. The selective neuronal NO synthase inhibitor 7-nitro-indazole blocks both long-term potentiation and depotentiation of field EPSPs in rat hippocampal CA1 *in vivo*. *J. Neurosci.* 16, 418–424 (1996).
27. Xu, L., Anwyl, R. & Rowan, M. J. Behavioural stress facilitates the induction of long-term depression in the hippocampus. *Nature* 387, 497–500 (1997).
28. Lenng, L. Behavior-dependent evoked potentials in the hippocampal CA1 region of the rat I. Correlation with behavior and EEG. *Brain Res.* 198, 95–117 (1980).
29. Moser, E., Mathiesen, I. & Andersen, P. Association between brain temperature and dentate field potentials in exploring and swimming rats. *Science* 259, 1324–1326 (1993).

Acknowledgements. This research was supported by the Health Research Board of Ireland, the European Union DGXII and the Wellcome Trust. We thank W. K. Cullen and J. Wu for assistance.

Correspondence and requests for material should be addressed to M.J.R. (e-mail: mrowan@tcd.ie).

Decreased lesion formation in CCR2$^{-/-}$ mice reveals a role for chemokines in the initiation of atherosclerosis

Landin Boring*†, Jennifa Gosling*, Michael Cleary* & Israel F. Charo*†‡

* *Gladstone Institute of Cardiovascular Disease, San Francisco, California 94141, USA*

† *Cardiovascular Research Institute, University of California, San Francisco, California 94110, USA*

‡ *Department of Medicine and the Daiichi Research Center, University of California, San Francisco, California 94110, USA*

Chemokines are proinflammatory cytokines that function in leukocyte chemoattraction and activation and have recently been shown to block the HIV-1 infection of target cells through interactions with chemokine receptors[1,2]. In addition to their function in viral disease, chemokines have been implicated in the pathogenesis of atherosclerosis. Expression of the CC chemokine monocyte chemoattractant protein-1 (MCP-1) is upregulated in human atherosclerotic plaques[3,4], in arteries of primates on a hypercholesterolaemic diet[5] and in vascular endothelial and smooth muscle cells exposed to minimally modified lipids[5,6]. To determine whether MCP-1 is causally related to the development of atherosclerosis, we generated mice that lack CCR2, the receptor for MCP-1 (ref. 7), and crossed them with apolipoprotein (apo) E-

null mice[9,10] which develop severe atherosclerosis. Here we show that the selective absence of CCR2 decreases lesion formation markedly in apoE$^{-/-}$ mice but has no effect on plasma lipid or lipoprotein concentrations. These data reveal a role for MCP-1 in the development of early atherosclerotic lesions and suggest that upregulation of this chemokine by minimally oxidized lipids is an important link between hyperlipidaemia and fatty streak formation.

The arterial fatty streak is composed of lipid-laden macrophages (foam cells) and is the precursor of more complex and dangerous lesions. The molecular signals that initiate monocyte/macrophage recruitment to the vessel wall are, however, unknown. We stained aortic root sections from mice on the Western diet[11] with MOMA-2, a macrophage-specific antibody[12]. Macrophages were abundant in the subendothelial space of CCR2$^{+/+}$,apoE$^{-/-}$ animals fed the high-fat diet for as little as 5 weeks, and constituted most of the cells in the lesion (Fig. 1a). In contrast, markedly fewer macrophages were present in the aortas of CCR2$^{-/-}$,apoE$^{-/-}$ mice (Fig. 1b). Quantitative analysis revealed significantly less MOMA-2-positive staining in CCR2$^{-/-}$ mice than in CCR2$^{+/+}$ mice (Fig. 1c). These data indicate that activation of CCR2 was important in recruitment of monocytes/macrophages into the vessel wall, the earliest recognizable sign of atherosclerosis. Staining with Oil Red O confirmed the significant decrease in lesion area in CCR2$^{-/-}$ mice fed the Western diet for 5 weeks (Fig. 2). Lesion size in the CCR2$^{+/-}$ mice was intermediate between the lesion sizes of wild-type and CCR2$^{-/-}$ mice, suggesting a gene dosage effect (Fig. 2). After 9 weeks on the diet, there was no difference between the CCR2$^{+/-}$ and wild-type mice, and both had significantly larger lesions than the CCR2$^{-/-}$ mice. The reduction in lesion size was observed throughout the aortic root and was most pronounced in the valve leaflet region, where wild-type mice developed the most severe lesions (not shown). After 13 weeks on the diet, CCR2$^{-/-}$ mice still had significantly smaller lesions than CCR2$^{+/-}$ mice (Fig. 2). Thus, lesion development was decreased at all time points examined. In addition, at both 9 and 13 weeks, the lesions were less complex in the CCR2$^{-/-}$ mice (not shown). These data suggest that the decreased recruitment of macrophages observed at 5 weeks reduced lesion size at the later time points.

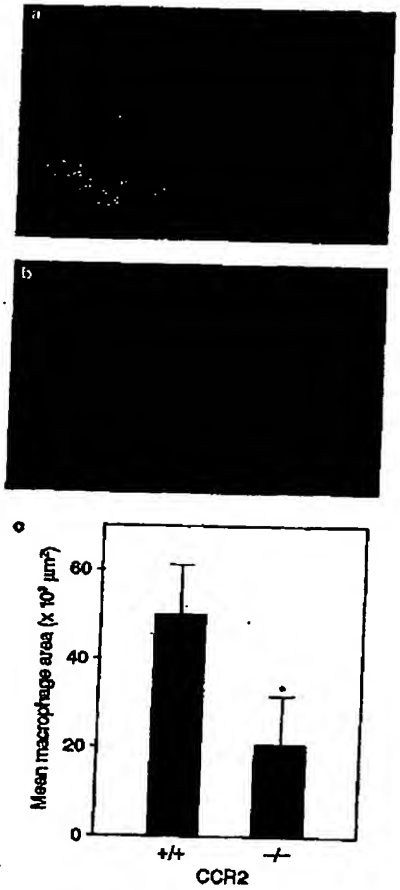

Figure 1 Macrophage infiltration of the aortic sinus in apoE$^{-/-}$ mice fed a high-fat (Western) diet for 6 weeks. **a**, CCR2$^{+/+}$; **b**, CCR2$^{-/-}$. Sections from the aortic sinus were stained for macrophages with MOMA-2 (red) and for nuclei with SYTOX green. Regions of overlap appear yellow. Shown are representative sections from mice of each genotype. Original magnification ×125. **c**, Quantitation of MOMA-2 staining. Values are means ± s.d. (n = six mice of each genotype). *P = 0.0043 for CCR2$^{+/+}$ versus CCR2$^{-/-}$ (Mann–Whitney test).

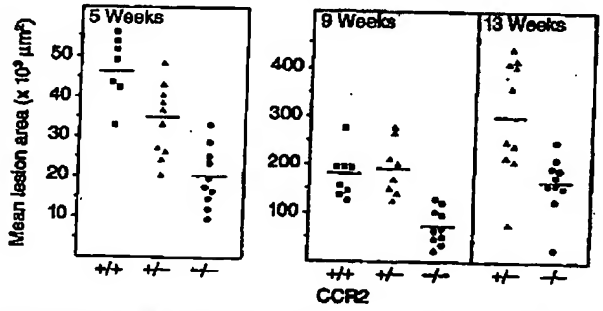

Figure 2 Mean lesion area in the aortic root. Cross-sections (10 μm) of the aorta were stained for lipid with Oil Red O and quantitated by digital morphometry. Each symbol represents one animal; bars represent means. Spearman rank order analysis suggested a gene dosage effect at the 5-week time point (r = 0.8028, P < 0.0001). For comparisons between groups, P < 0.001 for CCR2$^{+/+}$ versus CCR2$^{-/-}$ and P < 0.05 for CCR2$^{+/-}$ versus CCR2$^{-/-}$ at 5 weeks (ANOVA); P < 0.01 for CCR2$^{+/+}$ versus CCR2$^{-/-}$ and P < 0.001 for CCR2$^{+/-}$ versus CCR2$^{-/-}$ at 9 weeks (ANOVA); P = 0.0029 for CCR2$^{+/-}$ versus CCR2$^{-/-}$ at 13 weeks (Mann–Whitney test).

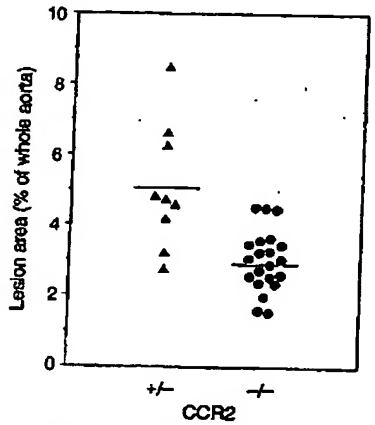

Figure 3 Lesion coverage in the aortas of CCR2$^{+/-}$ and CCR2$^{-/-}$ mice. Whole aortas from mice fed the high-fat diet for 13 weeks were mounted *en face* and stained for lipid with Sudan IV. Total lesion area from the aortic sinus to the femoral bifurcation was quantitated by digital morphometry. Each symbol represents one animal; bars represent means. The percentage of the aortic surface covered by lesions in the CCR2$^{-/-}$ mice (n = 21) was significantly lower than in the CCR2$^{+/-}$ mice (n = 9) (P = 0.001, Mann–Whitney test).

Table 1 Total cholesterol in serum from mice on the Western diet

Genotype	Total cholesterol (mg dl^{-1}) 6 weeks	9 weeks	13 weeks
CCR2$^{+/+}$,apoE$^{-/-}$	1916 ± 291 (17)	1947 ± 378 (8)	ND
CCR2$^{+/-}$,apoE$^{-/-}$	1809 ± 408 (20)	1963 ± 354 (11)	1978 ± 402 (10)
CCR2$^{-/-}$,apoE$^{-/-}$	1861 ± 431 (17)	1851 ± 613 (11)	1788 ± 376 (21)

Values shown are means ± s.d. (numbers of mice). ND, no data. Cholesterol levels were not significantly different between genotypes, $P = 0.1082$ for 6 weeks and $P = 0.8060$ for 9 weeks by ANOVA; $P = 0.1832$ for 13 weeks by Mann–Whitney test.

We next examined lesion development along the entire aorta in whole-mount *en face* preparations stained with Sudan IV. In animals on the Western diet for 5 and 9 weeks, less than 1% of the aorta was covered with lesions, and no significant differences between the CCR2 genotypes were observed (data not shown). At 13 weeks, however, lesions covered 5.1% of the aorta in the CCR2$^{+/-}$ mice, but only 2.9% in the CCR2$^{-/-}$ mice (Fig. 3). Thus, by two independent techniques, lesion size was significantly reduced in the absence of CCR2. Longer duration studies will be required to determine whether the size and complexity of the lesions in the CCR2$^{-/-}$ mice eventually equal those of the wild-type animals.

To determine whether differences in lipid metabolism could account for the decreased atherosclerosis in the CCR2$^{-/-}$ mice, we examined plasma lipid levels and lipoprotein profiles. Total serum cholesterol levels were not statistically different between the CCR2 genotypes at any time point and were within the range expected for apoE$^{-/-}$ mice maintained on this diet[11] (Table 1). In addition, no differences were observed in plasma triglyceride levels (285.6 ± 107.7 mg dl^{-1}, $n = 6$ for CCR2$^{+/+}$; 282.8 ± 86.4 mg dl^{-1}, $n = 5$ for CCR2$^{+/-}$; 307.2 ± 79.6 mg dl^{-1}, $n = 7$ for CCR2$^{-/-}$). As analysed by gel filtration chromatography, the plasma lipoprotein profiles were essentially identical in wild-type and CCR2$^{-/-}$ mice (Fig. 4). Consistent with earlier reports, most of the cholesterol in apoE$^{-/-}$ mice was contained within very-low-density lipoprotein-sized particles[8]. Lesion size in apoE$^{-/-}$ mice can be influenced by high-density lipoprotein (HDL) levels[10], but HDL cholesterol levels were very low and were unaffected by the CCR2 genotype (Fig. 4). These data suggest that the decreased lesion size in the CCR2$^{-/-}$ mice was not accounted for by changes in plasma cholesterol levels or in the distribution of lipoprotein particles. Gupta *et al.*[13] reported decreased atherosclerosis in interferon-γ receptor-deficient mice on the apoE$^{-/-}$ background and also noted an increase in plasma levels of apoA-IV, a potentially atheroprotective lipoprotein[14]. We found no difference in plasma apoA-IV concentrations between CCR2$^{+/+}$ and CCR2$^{-/-}$ mice (data not shown). The CCR2$^{-/-}$ mice were backcrossed with C57Bl/6 mice, resulting in study animals that were 87.5% C57Bl/6 and 12.5% 129/Sv. Although unlikely, the possibility that a 129/Sv gene contributed to the differences in atherosclerosis cannot be completely excluded, particularly if this gene was linked to CCR2.

In summary, these studies identify CCR2 as a genetic determinant of murine atherosclerosis and provide strong evidence for a direct non-cholesterol-mediated effect of MCP-1 in macrophage recruitment and atherogenesis. These results are consistent with those of Suzuki *et al.*[15], who reported a role for the macrophage scavenger receptor in atherosclerosis susceptibility. Monocytes also express CCR1 and CCR5, and atherosclerosis studies of mice in which multiple receptors have been genetically deleted will probably be of great interest. □

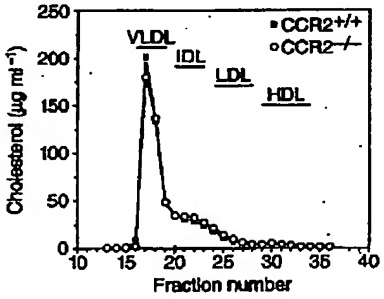

Figure 4 Lipoprotein profile of plasma from CCR2$^{+/+}$ and CCR2$^{-/-}$ mice. Values are averages of four mice of each genotype with similar total cholesterol levels. There were no significant differences in total non-HDL cholesterol (CCR2$^{+/+}$, 1,684 ± 161 mg dl^{-1}; CCR2$^{-/-}$, 1,510 ± 210 mg dl^{-1}) or HDL cholesterol (CCR2$^{+/+}$, 49 ± 27 mg dl^{-1}; CCR2$^{-/-}$, 64 ± 3.4 mg dl^{-1}) (Mann–Whitney). LDL, low-density lipoprotein; IDL, intermediate-density lipoprotein.

Methods

Genetically modified mice. CCR2$^{-/-}$ mice[7] (hybrids of C57Bl/6 and 129/SvJae) were mated with apoE$^{-/-}$ mice[9] on the C57Bl/6 background (N10 C57Bl/6, Jackson Labs). CCR2$^{+/-}$,apoE$^{+/-}$ mice were backcrossed with apoE$^{+/-}$ mice to produce CCR2$^{+/-}$,apoE$^{-/-}$ mice; these mice were intercrossed to produce all three CCR2 genotype on the apoE-null background (87.5% C57Bl/6; 12.5% 129/SvJae). The double-knockout (apoE$^{-/-}$,CCR2$^{-/-}$) mice were born at the expected Mendelian ratios, developed normally, and were disease-free while maintained in a pathogen-free environment. Mice were weaned at 4 weeks, fed normal rodent chow (4.5% fat; Ralston Purina Co.) for an additional week, and switched to the Western diet (21% fat, 0.15% cholesterol; Harlan Teklad no. 88137) at 5 weeks of age[11].

Quantification of atherosclerotic lesions. Hearts and aortas were prepared essentially as described[16,17], except that mice were perfused with 3.0% paraformaldehyde in PBS and tissues were equilibrated in 20% sucrose before embedding in OCT compound (Tissue Tek). Atherosclerosis was assessed by two independent techniques: Oil Red O staining of lesions in cross-sections from the aortic root and Sudan IV staining of lesions in pinned-out aortas. Cryosections (10 μm) spanning 550 μm of the proximal aorta were collected, and every fifth section, extending 250 μm in both directions from the coronary artery branch point, was stained with Oil Red O. Lesion areas were quantified with a digital colour video camera and Image-1/AT software as described[16]. Adjacent sections were stained with haematoxylin and eosin for morphological analysis. The remainder of the aorta was opened longitudinally along the ventral midline from the aortic root to the iliac arteries, and the lesion area in *en face* preparations stained with Sudan IV was quantitated as described[17]. Image analysis was performed by a trained observer blinded to the genotype of the mice.

Immunohistochemistry. Serial cryosections collected at 50-μm intervals were stained with a monoclonal rat antibody to the mouse monocyte–macrophage marker MOMA-2 (Biosource International, Camarillo, CA; 1:400 dilution), followed by detection with biotinylated secondary antibodies and streptavidin–horseradish peroxidase (PharMingen, San Diego). The signal was enhanced with the NEN DuPont Tyramide Signal Amplification kit, and sections were counterstained for nuclei with SYTOX green (Molecular Probes, Eugene, OR). Fluorescent images were captured into Image-1 as described above. Data represent the average area of MOMA-2 staining from 6–8 sections per mouse.

Lipid analysis. Cholesterol and triglyceride concentrations were determined with colorimetric assay kit (Spectrum cholesterol kit, Abbott Labs; GPO triglyceride kit, Boehringer Mannheim). Cholesterol levels were measured in serum of nonfasted mice collected at the time of killing, and triglycerides were assayed in plasma obtained after a 4-h fast. For lipoprotein analysis, plasma was prepared from blood collected by retro-orbital puncture into tubes containing EDTA (1 mM) and aprotinin (1.3×10^3 U ml^{-1}, ICN). Plasma samples from individual mice (50 μl in a total volume of 300 μl) were fractionated by FPLC on a Superpose 6 column (HR 10/30, Pharmacia LKB) as described[18]. ApoA-IV levels in plasma were determined by gradient gel electrophoresis (SDS–PAGE, 4–15% Tris-HCl Ready Gel; Bio-Rad) of very-low-density lipoprotein (fractions 17–19; Fig. 4) from four CCR2$^{+/+}$ and four CCR2$^{-/-}$ mice, followed by western blot analysis with a rabbit polyclonal antibody against rat apoA-IV (generously provided by Karl Weisgraber, Gladstone Institute of Cardiovascular Disease).

Statistical analysis. For analysis of lesion size, comparisons between groups were performed using the Kruskal–Wallis nonparametric ANOVA or Mann–

Whitney *U* test. The Spearman rank order correlation was used to analyse the relationship between CCR2 gene dosage and lesion area. Instat 2.01 software for the Macintosh was used for all calculations.

Received 11 May; accepted 9 July 1998.

1. Cocchi, F. *et al.* Identification of RANTES, MIP-1α, and MIP-1β as the major HIV-suppressive factors produced by CD8⁺ T cells. *Science* **270**, 1811–1815 (1995).
2. Choe, H. *et al.* The β-chemokine receptors CCR3 and CCR5 facilitate infection by primary HIV-1 isolates. *Cell* **85**, 1135–1148 (1996).
3. Nelken, N. A., Coughlin, S. R., Gordon, D. & Wilcox, J. N. Monocyte chemoattractant protein-1 in human atheromatous plaques. *J. Clin. Invest.* **88**, 1121–1127 (1991).
4. Yla-Herttuala, S. *et al.* Expression of monocyte chemoattractant protein 1 in macrophage-rich areas of human and rabbit atherosclerotic lesions. *Proc. Natl Acad. Sci. USA* **88**, 5252–5256 (1991).
5. Yu, X. *et al.* Elevated expression of monocyte chemoattractant protein 1 by vascular smooth muscle cells in hypercholesterolemic primates. *Proc. Natl Acad. Sci. USA* **89**, 6953–6957 (1992).
6. Cushing, S. D. *et al.* Minimally modified low density lipoprotein induces monocyte chemotactic protein 1 in human endothelial cells and smooth muscle cells. *Proc. Natl Acad. Sci. USA* **87**, 5134–5138 (1990).
7. Boring, L. *et al.* Impaired monocyte migration and reduced type 1 (Th1) cytokine responses in C-C chemokine receptor 2 knockout mice. *J. Clin. Invest.* **100**, 2552–2561 (1997).
8. Plump, A. S. *et al.* Severe hypercholesterolemia and atherosclerosis in apolipoprotein E-deficient mice created by homologous recombination in ES cells. *Cell* **71**, 343–353 (1992).
9. Zhang, S. H., Reddick, R. L., Piedrahita, J. A. & Maeda, N. Spontaneous hypercholesterolemia and arterial lesions in mice lacking apolipoprotein E. *Science* **258**, 468–471 (1992).
10. Plump, A. S., Scott, C. J. & Breslow, J. L. Human apolipoprotein A-I gene expression increases high density lipoprotein and suppresses atherosclerosis in the apolipoprotein E-deficient mouse. *Proc. Natl Acad. Sci. USA* **91**, 9607–9611 (1994).
11. Nakashima, Y., Plump, A. S., Raines, E. W., Breslow, J. L. & Ross, R. ApoE-deficient mice develop lesions of all phases of atherosclerosis throughout the arterial tree. *Arterioscler. Thromb.* **14**, 133–140 (1994).
12. Kraal, G., Rep, M. & Janse, M. Macrophages in T and B cell compartments and other tissue macrophages recognized by monoclonal antibody MOMA-2. An immunohistochemical study. *Scand. J. Immunol.* **26**, 655–661 (1987).
13. Gupta, S. *et al.* IFN-γ potentiates atherosclerosis in apoE knock-out mice. *J. Clin. Invest.* **99**, 2752–2761 (1997).
14. Duverger, N. *et al.* Protection against atherogenesis in mice mediated by human apolipoprotein A-IV. *Science* **273**, 966–968 (1996).
15. Suzuki, H. *et al.* A role for macrophage scavenger receptors in atherosclerosis and susceptibility to infection. *Nature* **386**, 292–296 (1997).
16. Purcell-Huynh, D. A. *et al.* Transgenic mice expressing high levels of human apolipoprotein B develop severe atherosclerotic lesions in response to a high-fat diet. *J. Clin. Invest.* **95**, 2246–2257 (1995).
17. Virtanen, M. M. *et al.* Susceptibility to atherosclerosis in mice expressing exclusively apolipoprotein B48 or apolipoprotein B100. *J. Clin. Invest.* **100**, 180–189 (1997).

Acknowledgements. We thank D. Sansa, D. Newland and L. Jensen for help with tissue preparation and staining; D. Dichek for advice on statistical analysis; J. C. W. Carroll, N. C. Shea and S. Gonzales for figure preparation; J. Ernst for assistance with fluorescent microscopy; G. Howard and S. Ordway for editorial expertise and A. Chen for manuscript preparation. We also thank B. Pitas, R. Furze and K. Weisgraber for careful readings of the manuscript. This work was supported in part by a grant from the NIH to J.P.C.

Correspondence and requests for materials should be sent to J.P.C. at the Gladstone Institute of Cardiovascular Disease (e-mail: ichaw@gladstone.ucsf.edu).

Leptin modulates the T-cell immune response and reverses starvation-induced immunosuppression

Graham M. Lord*†, Giuseppe Matarese*†‡, Jane K. Howard†§, Richard J. Baker*, Stephen R. Bloom§ & Robert I. Lechler*

*Imperial College School of Medicine, Departments of *Immunology and §Endocrinology, The Hammersmith Hospital, Du Cane Road, London W12 0NN, UK*

† *These authors contributed equally to this work.*

Nutritional deprivation suppresses immune function[1–3]. The cloning of the *obese* gene and identification of its protein product leptin[4] has provided fundamental insight into the hypothalamic regulation of body weight[5,6]. Circulating levels of this adipocyte-derived hormone are proportional to fat mass[6,7] but may be lowered rapidly by fasting[8,9] or increased by inflammatory mediators[10,11]. The impaired T-cell immunity of mice[12,13] now known to be defective in leptin (*ob/ob*)[4] or its receptor (*db/db*)[14,15], has never been explained. Impaired cell-mediated immunity[1–3] and reduced levels of leptin[7] are both features of low body weight in humans. Indeed, malnutrition predisposes to death from infectious diseases[16]. We report here that leptin has a specific effect on T-lymphocyte responses, differentially regulating the proliferation of naive and memory T cells. Leptin increased Th1 and suppressed Th2 cytokine production. Administration of leptin to mice reversed the immunosuppressive effects of acute starvation. Our findings suggest a new role for leptin in linking nutritional status to cognate cellular immune function, and provide a molecular mechanism to account for the immune dysfunction observed in starvation.

Most immune responses are orchestrated by $CD4^+$ helper T cells (Th). We first determined the effect of leptin on Th responses in the context of the mixed-lymphocyte reaction (MLR) resulting from the culture of T cells with major histocompatibility complex (MHC)-incompatible (allogeneic) stimulator cells. The doses of leptin used in these experiments were chosen to incorporate the range of serum levels measured in humans[17]. Leptin induced a

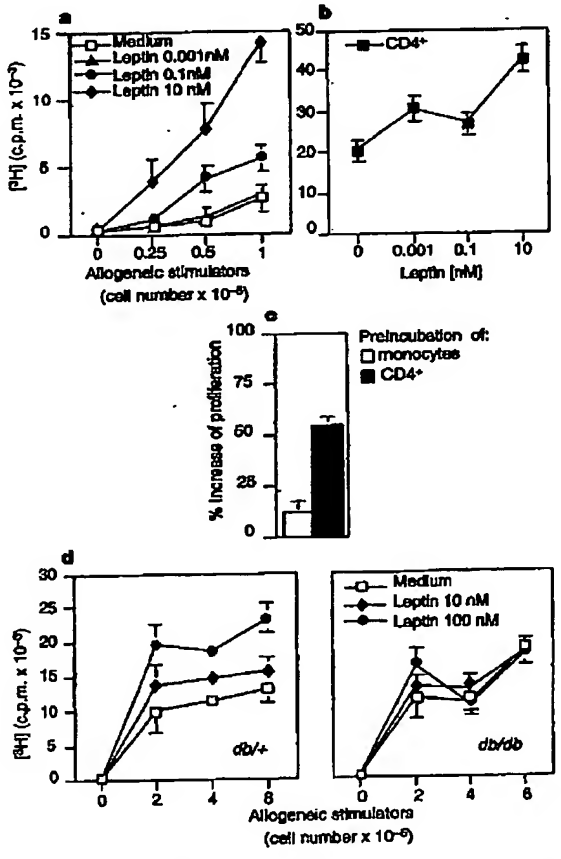

Figure 1 Leptin enhances the alloproliferative response. **a**, **b**, Thymidine incorporation in the presence of leptin in an MLR performed using human PBLs as responder and MHC-mismatched PBMCs as stimulator cells (**a**) or highly purified $CD4^+$ T cells as responders as a responder/stimulator ratio of 1:1 (**b**) (8 experiments). **c**, Preincubation of either responder $CD4^+$ T cells or irradiated stimulator allogeneic monocytes with 10 nM leptin before co-culture in the absence of leptin. **d**, MLR using murine heterozygous *db/+* ($H\text{-}2^d$) and homozygous *db/db* ($H\text{-}2^d$) splenocytes as responders with irradiated C57BL/6 ($H\text{-}2^b$) allogeneic splenocytes (3 experiments). All data are expressed as mean c.p.m. of triplicate cultures ± s.e.m.

‡ Present address: Laboratorio di Immunologia, Dipartimento di Biologia e Patologia Cellulare e Molecolare, Università di Napoli "Federico II", via Pansini 5, 80131, Napoli, Italy.